Xylenes Reactions and Diffusions in ZSM-5 Zeolite based Catalyst

S. Al-Khattaf*

Department of Chemical Engineering
King Fahd University of Petroleum & Minerals
Dhahran 31261, Saudi Arabia.

Abstract

Xylenes transformations have been investigated over ZSM-5 zeolite in a riser simulator that mimics closely the operation of commercial fluidized-bed reactors. P-xylene was found to be more reactive than the other isomers followed by o-xylene and m-xylene was found to be least reactive. The order of reactivity is consistent with the order of diffusivity. At low temperature (400°C), isomerization and disproportionation yields for all xylenes were found equal at constant conversion. However, as reaction temperature increases to 500°C, m-xylene reaction will be more selective to disproportionation than other xylene isomers. The effectiveness factor for all xylene isomers reactions was found based on two different diffusivities used from the literature. Generally m-xylene effectiveness factor was estimated to be less than 0.1 indicating to a high diffusion obstacle inside ZSM-5 zeolite. While o-xylene was found to have effectiveness factor in a range of 0.35-0.45, p-xylene effectiveness factor was found to be close to unity indicating no diffusion limitation.

Keywords: Xylene transformation, Kinetic modeling, fluidized-bed reactor, ZSM-5, isomerization, disproportionation, effectiveness factor, Thiele modulus.

*Corresponding author. Tel.: +966-3-860-1429; Fax: +966-3- 860-4234
E-mail address: skhattaf@kfupm.edu.sa

1. Introduction

With increasing demand for p-xylene as starting materials for the manufacture of synthetic fibres (polyester), efforts are continually being directed to selectively produce p-xylene from low valued m-xylene. Unfortunately, the amount of p-xylene theoretically obtainable from these aromatic compounds is very much limited by thermodynamics. Consequently, attempts to overcome thermodynamic limitations in the transformation of xylenes have indeed constituted a great challenge to both the academic field and petrochemical industry. However, the introduction of ZSM-5 for xylene transformation process by Mobil workers in the early 1970s represented a clear technological improvement.

Xylene isomerization can occur via two mechanisms; unimolecular isomerization and bimolecular isomerization [1-4]. Corma and Sastre [3] indicated that bimolecaular mechanism is crucial in large pore zeolite like H-Y and mordinite. Guisnet and coworkers [4] estimated 20 % of the isomerization in Y-zeolite is coming via the bimolecular isomerization. Recently it was shown that m-xylene isomerization over ZSM-5 zeolite can take place via both 1,2 methyl shift and 1,3 methyl shift [5]. Furthermore, it has been reported that the bimolecular isomerization over Y-zeolite has P/O ratio of 0.275 [4] which is essentially different from the value of 1.18 for the unimolecular isomerization [6]. Thus the low P/O can be attributed to the increased bimolecular isomerization. Zheng et al.[7] reported a P/O ratio of approximately 2.0 over tetra-ethoxysilane modified HZSM-5, leading to an enhanced *p*-xylene selectivity. A similar P/O ratio has also been obtained by Llopis et al.[8] via molecular dynamics simulation over ZSM-5.

Shape selective conversion of xylenes over ZSM-5 has been investigated in detail by several workers [9-19]. Li et al. [13] used a pulse microreactor-chromatograph technique to study the xylene isomerization reaction over HZSM-5 zeolite catalyst. Their reported activation energies indicated that the transformation of m-xylene to o- or p-xylene, o-xylene to m- or p-xylene, and p-xylene to toluene are controlled by reaction, and the conversion of p-xylene to m- or o-xylene is in the transition regime of diffusion and reaction. Ma and Savage [14] also studied xylene isomerization over ZSM-5 to observe the

effects of site modification on the reaction. The kinetic, diffusion, and adsorption parameters they determined were generally in agreement with literature.

Shape-selectivity concept was introduced by Weisz and Frilette [20] and experimentally explained by Garcia and Weisz [21]. Diffusivity in ZSM-5 is considerably affected by the molecular size and structure. Thus ZSM-5 small pores can lead to a sharp screening of either reactants or products according to the ease of diffusivity of these molecules. In these zeolites, intracrystalline diffusion plays a significant role in deciding reactant conversion and product selectivity. For example, p-xylene formed by the catalytic reaction can easily escape via the ZSM-5, while the other isomers further isomerize to more mobile molecule (p-xylene) [22]. Wei [22] presented a quantitative diffusional theory of para-selectivity and a ratio of diffusivities 1:1:1000 for o:m:p respectively. As a result of its strong shape selectivity, ZSM-5 is a suitable catalyst for the synthesis of alkyl and di-alkyl benzenes, particularly their para-isomers[23]. Thus p-xylene isomerization is well known and it is used as a test reaction for shape selective zeolite [24] .

Warner et al [25] attributed the variation in selectivity to the large differences in the diffusivities of the variously-sized molecular species in the zeolite structure. Thiele modulus relates the conversion of certain molecule to diffusion. Chutoranski and Dwyer [26] indicated the significance of zeolite crystal size in the xylene isomerization reaction. Chen et al [27] observed improvement in p-xylene selectivity in the methylation of toluene when large ZSM-5 crystals were used.

One of the most challenging tasks in calculating Thiele modulus and the effectiveness factor is to find a reasonable approximation for the diffusivity. Choudhary and Akolekar [28] studied the effect of diffusion on cracking of isooctane over ZSM-5. A very small zeolite crystal was used to estimate the intrinsic rate constant. Then, a relatively large zeolite crystal was used to estimate the apparent rate constant. The effectiveness factor was experimentally obtained. The effective diffusivity was then estimated from the knowledge of Thiele Modulus (which was obtained from the experimental measurement of the effectiveness factor). However, they found a tremendous difference between measured isoocatane diffusivity in non-reacting system by GC pluse technique and the diffusivity that is calculated based on the experimentally obtained effectiveness factor. Warner et al [24] estimated the effectiveness factor of several hydrocarbons (non-aromatics) in ZSM-5. They

reported an effectiveness factor of 1 for normal paraffins and less than one for branched molecules. The effectiveness factor was found based on the ratio of the observed rate constant based on large zeolite crystal) over the intrinsic rate constant (based on a very small zeolite crystal). Diffusivity is then found based on the approximated effectiveness factor and Thiele Modulus.

Al-Khattaf et al [29] estimated Thiele Modulus and effectiveness factor of 1,3,5 triisopropylbenzene (1,3,5 TPB) and recently for 1,2,4 trimethyl benzene [30] based on the estimated diffusivity of these molecules that have been reported in the literature. Hedlund et al. [31] developed a reaction-diffusion model for p-xylene over ZSM-5. They used two different set of ratios between the diffusivities of p-xylene, o-xylene and m-xylene to calculate the effectiveness factor of thin ZSM-5 films. The first set of ratio was based on that p-xylene diffusivity (D_P) = 1000 times that of o-xylene (D_O) and that of m-xylene (D_M) and the second set of ratios was reported by Mirth et al [32] and that $D_P = 0.01D_O = 0.001D_M$. This ratio will be used in our effectiveness factor calculation along with Han et al data for p-xylene diffusivities [33]. On the other hand, Choudary et al measured the liquid phase diffusivities of the three xylenes isomers over ZSM-5 [34].

The present study is aimed at modeling the kinetics of the three xylenes isomers transformation over ZSM-5 in a fluidized-bed reactor using the "time on stream" decay model. An attempt will be made to compare the reactivity and diffusivity of the three xylenes isomers over ZSM-5 based catalyst. The modeling procedure will take into consideration the different diffusion rate for all xylene isomers. The xylenes transformation will be carried out in a riser simulator that resembles closely the operation of commercial fluidized bed reactors. Furthermore, the effect of reaction conditions on the different xylene ratios i.e., p-xylene/o-xylene (P/O) ratio, p-xylene/m-xylene (P/M) ratio, and m-xylene/o-xylene (M/O) will be investigated.

2. Experimental Section

2.1 The riser simulator

All the experimental runs were carried out in the riser simulator. This reactor is novel bench scale equipment with internal recycle unit invented by de Lasa [35] to overcome the

technical problems of the standard micro-activity test (MAT). For example, the low olefinity obtained from MAT reactor, due to its higher reaction time (> 75 s) as compared to the riser (< 15 s), non uniform coke deposition (150 mm long catalyst bed), and temperature/concentration gradient, which are eliminated by the well-mixed characteristics and intense fluidization of the riser simulator. The riser simulator is fast becoming a valuable experimental tool for reaction evaluation involving model compounds [36,37] and also for testing and developing new fluidized catalytic cracking in vacuum gas oil cracking[38].

The riser simulator consists of two outer shells, the lower section and the upper section, which allow one to load or to unload the catalyst easily, as illustrated in Fig. 1. The reactor was designed in such a way that an annular space is created between the outer portion of the basket and the inner part of the reactor shell. A metallic gasket seals the two chambers with an impeller located in the upper section. A packing gland assembly and a cooling jacket surrounding the shaft provide support for the impeller. Upon rotation of the shaft, gas is forced outward from the center of the impeller toward the walls. This creates a lower pressure in the center region of the impeller, thus inducing flow of gas upward through the catalyst chamber from the bottom of the reactor annular region where the pressure is slightly higher. The impeller provides a fluidized bed of catalyst particles as well as intense gas mixing inside the reactor. A detailed description of various riser simulator components, sequence of injection and sampling can be found in work by Kraemer [39].

2.2 Materials

The as-prepared ZSM-5 zeolite used in this work was spray-dried using kaolin as the filler and a silica sol as the binder. The resulting 60 μm catalyst particles had the following composition: 30 wt % zeolite, 50 wt % kaolin, and 20 wt % silica. The catalyst was calcined at 600^{o}C for 2 h.

Analytical grade (99% purity) pure p-xylene, *m*-xylene, and o-xylene were obtained from Fluka. All chemicals were used as received as no attempt was made to further purify the samples.

2.3 Catalyst characterization

The BET surface area was measured according to the standard procedure ASTM D-3663 using Sorptomatic 1800 Carlo Erba Strumentazione unit, Italy. The unit cell size was determined by X-ray diffraction following ASTM D-3942-80 procedure. The acid property of the catalyst was characterized by NH_3 temperature-programmed desorption (NH_3-TPD). In all the experiments, 50 mg of sample was outgassed at 400^oC for 30 min in flowing He and then cooled down to 150^oC. At that temperature, NH_3 was adsorbed on the sample by injecting pulses of 2 µl/pulse. The injection was repeated until the amount of NH_3 detected was the same for the last two injections. After the adsorption of NH_3 was saturated, the sample was flushed at 150^oC for 1 h with He to remove excess NH_3, and then the temperature was programmed at 30 ^oC/min up to 1000^oC in flowing He at 30 ml/min. Flame ionization detector was used to monitor the desorbed NH_3.

2.4. Procedure

The experimental procedure in the riser simulator may be summarized as follows; a 80 mg portion of the catalyst was weighed and loaded into the riser simulator basket. The system was then sealed and tested for any pressure leaks by monitoring the pressure changes in the system. Furthermore, the reactor was heated to the desired reaction temperature. The vacuum box was also heated to around 250^oC and evacuated at around 0.5 psi to prevent any condensation of hydrocarbons inside the box. The heating of the riser simulator was conducted under continuous flow of inert gas (Ar), and it usually takes a few hours until thermal equilibrium is finally attained. Meanwhile, before the initial experimental run, the catalyst was activated for 15 min at 620^oC in a stream of Ar. The temperature controller was set to the desired reaction temperature, and in the same manner, the timer was adjusted to the desired reaction time. At this point the GC is started and set to the desired conditions.

Once the reactor and the gas chromatograph have reached the desired operating conditions, the feedstock was injected directly into the reactor via a loaded syringe. After the reaction, the four-port valve immediately opens, ensuring that the reaction was terminated and the entire product stream sent online to the analytical equipment via a preheated vacuum box chamber.

2.5 Analysis

The riser simulator operates in conjunction with a series of sampling valves that allow, following a predetermined sequence, one to inject reactants and withdraw products in short periods of time. The products were analyzed in an Agilent 6890N gas chromatograph with a flame ionization detector and a capillary column INNOWAX, 60-m cross-linked methyl silicone with an internal diameter of 0.32 mm.

3. Kinetic Model Development

The riser simulator being a constant volume batch reactor unit, operated isothermally, a suitable material balance equation that describes reactant disappearance is given by Al-Khattaf and de Lasa [36] as:

$$-\frac{V}{W_{cr}}\frac{dC_A}{dt} = \eta_{ss} r_A \qquad (1)$$

where C_A is the reactant concentration in the riser simulator; V the volume of the reacting mixture; W_{cr} the mass of the catalysts in the reacting system; η_{ss} an effectiveness factor to account for the influence of the pore diffusion resistance on the overall reaction rate; and r_A the reaction rate.

Considering that the disappearance of xylene isomers follows a first order kinetics, eq 1 can be expressed as:

$$-\frac{V}{W_{cr}}\frac{dy_A}{dt} = \eta_{ss} k_{A,in} \varphi_{in} y_A \qquad (2)$$

Where y_A is the mass fraction of species A, $k_{A,in}$ is the intrinsic kinetic parameter, and φ_{in} is the intrinsic decay function that takes into account the deactivation of the catalyst.

A classical approach while describing catalyst decay is to consider catalyst decay as function of time-on-stream. A classical relationship is the one proposed by Voorhies [40]:

$$\varphi = \exp(-\alpha t) \qquad (3)$$

where α is a constant and t is the time the catalyst is exposed to a reactant atmosphere (time–on-stream [TOS]). Considering that $k_{A,in}$ can be redefined as $k_{A,in} = k_0^{'} \times \exp\left[-E_R / R\left(1/T - 1/T_0\right)\right]$, eq 2 can be rewritten as follows:

$$-\frac{V}{W_{cr}}\frac{dy_A}{dt} = \eta_{ss} k_0^{'} \exp\left[\frac{-E_R}{R}\left(\frac{1}{T} - \frac{1}{T_0}\right)\right] \exp\left(-\alpha t\right) y_A \qquad (4)$$

The effectiveness factor (η_{ss}) expresses the extent of diffusional constraints inside a catalyst. For a zeolite crystal under steady state, η_{ss} is defined as the ratio of the actual reaction rate to the reaction rate in the absence of internal diffusional resistance.

$$\eta_{ss} \approx \frac{\tanh\left(h^{'}\right)}{h^{'}} \qquad (5)$$

Where $h^{'}$ is the modified Thiele Modulus, defined as;

$$h^{'} = \frac{1}{a_{ext}} \sqrt{\frac{k_{A,in} \rho_{cr} \varphi_{in}}{D_{eff}}} \qquad (6)$$

with a_{ext} being the specific external surface area for the zeolite crystal (a_{ext}=6/D_{cr}), D_{eff} the effective diffusivity, and ρ_{cr} is the zeolite density (825 kg/m^3). The effective diffusivity coefficient in zeolites can be represented as:

$$D_{eff} = D_0 \exp\left(-\frac{E_D}{RT}\right) \qquad (7)$$

where E_D represents the diffusion activation energy.

Eq 7 is very useful in estimating temperature effect on reactant transport. Choudhary et al [34] estimated the diffusivity parameters for each isomer in ZSM-5. However, their work was based on liquid phase diffusivity for low temperature range of

313-360 K. Therefore, when their diffusivities were used in equation 7, effectiveness factors resulted were too low for m-xylene, and o-xylene and p-xylene were having equal effectiveness factor which was not accepted. On the other hand, Han et al.[33] measured the p-xylene diffusivity in ZSM-5 at higher temperature range. Based on the experimental results reported by Han et al.[30] for p-xylene diffusivity over ZSM-5 crystals in the temperature range of 373-473K, energy of activation of 1.85 kcal/mol and $D_O = 4.9 \times 10^{-12}$ m^2/s were estimated by the authors. Mirth et al [32] investigated diffusion and reaction of xylenes over ZSM-5 zeolite and found that the difference in diffusion coefficients determined for the three xylene isomers (p:o:m = 1000:10:1). Similar ratios were also reported by Choudhary and Akolekar [40].These ratios are close to other reported in literature, for example Wei [22] and Chen [41] reported that diffusion rate of p-xylene in ZSM-5 is 1000 time faster than that of other isomers where diffusion coefficients are in the following ratios p:o:m = 1000:1:1. Furthermore, Roque-Malherbe and Ivanov [42] reported that p-xylene diffusivity is 25 times higher than that of o-xylene at 152°C over the 10 MR ZSM-11. Therefore, the ratios obtained by Choudhary and Akolekar [40] and Mirth et al [32] will be used in the present study. Table 1a reports the diffusivities parameters taken from Choudhary et al [34] and Han et al.[33]. Table 1b reports the diffusivities of p-xylene and o-xylene at 400 and 500°C calculated based on Choudhary et al [34] parameters. These diffusivities will be very useful for the result discussion.

Therefore, catalytic conversion of the methyl benzenes in the riser simulator can be modeled using a set of two equations, namely, eqs 4 and 5. Since the diffusion parameters (D_O and E_D) are known, only three intrinsic kinetic parameters ($k_0^{'}$, E_R, and α) need to be determined to fully characterize the diffusive- reactive system.

4. Results and Discussion

4.1 Catalyst characterization

Zeolite catalysts for use in fluidized-bed reactors are often incorporated in amorphous matrix to achieve the desired fluidization of the catalyst particles. As a result, the determination of the crystallinity and phase purity of the zeolite samples in the presence of this matrix is important in catalytic reactions. The XRD patterns of the ZSM-5 catalysts obtained are in agreements with those reported in the literature, without the presence of

extraneous peaks. The amount of desorbed NH_3 (total acidity) is 0.233 mmol/g. Finally, the measured BET surface area is 70 m^2/g.The detailed characterization results have been reported in ref. 5.

4.2 Xylenes conversion

The conversion of xylene isomers are shown for each xylene in Fig. 2a and 2b at 400^{o}C and 500^{o}C respectively. It can be seen from these figures that p-xylene converts to other products more rapidly than the other two xylene isomers. Also, the conversion of o-xylene can be seen to be higher than m-xylene at all reaction temperatures and times studied. This is in agreement with the diffusivity of the xylenes over ZSM-5 zeolite which was found to decrease in the following sequence: p-xylene > o-xylene > m-xylene as shown by Mirth et al [32]. Furthermore, Armaroli et al [43] noticed that the access of m-xylene to ZSM-5 structure is more hindered than that of o-xylene.

P-xylene has been found to be always more reactive than the others followed by o-xylene then m-xylene. This is expected since p-xylene mobility inside ZSM-5 is much greater than the other xylene isomers. The maximum conversion obtained for all xylenes was achieved at 500°C and 15 sec contact time as follows: 30.5 % for m-xylene; 37.5 % for o-xylene and 42.5 % for p-xylene. While at 400°C and 15 sec contact time, these conversions become 19.5 % for m-xylene; 22.5 % for o-xylene and 32 % for p-xylene. It can be noticed that at 400°C, o-xylene conversion is close to m-xylene conversion. However, as temperature increases to 500°C the difference between the conversions of these two isomers becomes more noticeable. The reason for this behaviour is probably that *o*-xylene diffusivity is more affected with rise in temperature than that of *m*-xylene. The transport of m-xylene is apparently more hindered than that of *o*-xylene at 500°C [43]. Similar sequence for xylene isomers reactivity over ZSM-5 was reported by Mirth et al [32]. They reported that the reaction rate of the xylene isomers at 300°C decreased in similar sequence as found in the present study. Furthermore, they reported an effectiveness factor of 0.5 for o-xylene isomerization over ZSM-5 at 250°C.

In order to explain the trend in the sequence of reactivity of the xylenes over ZSM-5 used in this study, the difference in the diffusion and adsorption of the xylene isomers over ZSM-5 should be considered. With ZSM-5 zeolite, the decrease in the reactivity of the

xylenes: p-xylene > o-xylene > m-xylene, demonstrates diffusional discrimination between the xylene reactants (reactant selectivity). Indeed, it has been established that the ratio of diffusion coefficient for *p* : *o* : *m* is 1000 : 100 : 1, respectively [32,40]. As a result, p-xylene with the smallest molecular diameter diffuses faster inside the pore of ZSM-5, and thus is more accessible to the active sites as compared to the bulkier o- and m-xylenes. Furthermore, Mirth et al. [32] has reported that pronounced difference exists in the adsorption rate and surface coverage of xylenes under non steady state conditions (similar to the condition of this study) over ZSM-5. With p-xylene reactant, adsorption-desorption equilibrium was achieved within a few seconds, while it was achieved within a few minutes with o-xylene and after 5 min for m-xylene reactant at 300^{o}C. Furthermore, the low m-xylene reactivity compared to the other xylene isomers can be due to the low Brönsted acid site coverage compared to the other xylenes. It has also been reported that while complete coverage of Brönsted acid site for the p-xylene and o-xylene is achieved, only 65-70% of Brönsted acid site are covered when m-xylene is used as reactant [32]. These results, along with diffusion rate of each xylene isomer in ZSM-5, perfectly explain the observed trend in the reactivity of the xylenes obtained in the present study. Thus, it is clear that the transformation of xylenes (especially m-xylene) over ZSM-5 zeolite is in the transition regime of diffusion and reaction. Collins et al [44] investigated the reactivity of the three xylene isomers over ZSM-5 at 300°C. While m-xylene was found to have the lowest reactivity, p-xylene and o-xylene were found to have similar reactivity.

4.2 Products distribution

The transformation of xylenes proceeds via two major reaction pathways over zeolite catalysts: isomerization and disproportionation pathways. The products of the transformations of the three xylene isomers are shown in Tables 2-4. As shown in these tables, the major reaction products of each xylene reactants are: the other two xylene isomers, trimethylbenzenes and toluene.

4.2.1 Xylene Isomerization (I)

The isomerization of each xylene yields the other two isomers. These two isomers are related thermodynamically with each other. At low temperature 400°C, the isomerization

yield versus conversion is shown at Fig.3a. It can be seen from this figure that isomerization is a primary reaction and at same conversion each isomer has similar isomerization selectivity. However, this trend is different when temperature has been raised to 500°C. Figure 3b shows that m-xylene has lower isomerization selectivity than both o-xylene and p-xylene which are located on the same line.

Regarding P/O ratio, ZSM-5 was shown to have a ratio which is greater than the equilibrium value (around 1.0). Due to the high diffusivity of p-xylene (1000 times higher than that of m-xylene and 100 times higher than that of o-xylene), it can leave ZSM-5 structure as soon it forms. However, o-xylene diffusivity is much slower than that of p-xylene especially at low reaction temperature. Therefore, o-xylene might be forced to transform to smaller molecule in order to be able to leave the zeolite structure [45]. Several P/O ratios over ZSM-5 were reported in the literature. Jones et al [6] and Martens et al [46] reported a value of 2.8 for the P/O ratio while Collins et al [44] obtained 1.35 P/O ratio at 300°C. This behavior decreases with temperature due to great influence of temperature on the configrational diffusion of o-xylene. As shown in Fig 4a, the P/O ratio is greater than equilibrium value which is about 1. The ratio is shown to decrease with temperature. The highest P/O was found at 400°C and 15 sec reaction time to be around 1.8 which is close to the value of around 2 reported by Mirth et al [32,47] at a temperature range of 250-300°C. In ref. 47, the selectivity of *m*-xylene isomerization is explained by restrictions to the transition state to form *o*-xylene. In the case of *p*- and *o*-xylene isomerization, the selectivity is controlled by restrictions of the transport of the primary product *m*-xylene out of the pores. However, it was noticed that this ratio decreases with temperature reaching a minimum value of 1.2 at 500°C. This behavior can be easily explained based on the diffusivity of both p-xylene and o-xylene. It seems that at 500°C the difference in diffusion rate of both p-xylene and o-xylene decreases leading to decrease P/O ratio to a value close to unity. The results of conversion of each isomer support this assumption. Fig 2a (at 400°C) shows large difference in conversion between o-xylene and p-xylene, whereas this difference has decreased when temperature was raised to 500°C. Hsu et al [45] has reported opposite trend for P/O with temperature over Pt-ZSM-5. It was shown that P/O was highest at 300°C and lowest at 400°C. Furthermore, Iliyas and Al-Khattaf have not noticed a

significant role of temperature on P/O ratio when USY zeolite was used [48]. No diffusion resistance was expected in xylene isomerization over fujasite zeolite [14].

P-xylene isomerization produces both m-xylene and o-xylene. The equilibrium ratio as shown in Fig 4b is around 2. However, we notice that M/O ratio is much larger than the equilibrium ratio and it could reach 4 at 400°C reaction temperature. Mirth et al [29] reported a M/O ratio of around 5 at a temperature range of 250-300°C and a M/O ratio of 2.6 was obtained by Collins et al [44]. It was also noticed that this ratio decreases with temperature and it is not significantly affected by conversion. For example, at 500°C this ratio decreased up to 3. Similar behavior was reported earlier over USY zeolite [48]. These results can be attributed to 1,2 shift and 1,3 shift mechanisms. P-xylene can not transform directly (via 1,2 shift) into o-xylene. It has to first transform into m-xylene, then m-xylene can isomerize further into o-xylene. Based on this, M/O ratio is higher than the equilibrium value especially at 400°C. At 500°C the 1,3 shift mechanism rate increases [5], more o-xylene can be produced at higher temperature leading to a decrease in M/O from 4 to 3.

Fig 4c shows that M/P ratio is close to the equilibrium value 2. Mirth et al [32] reported an M/P ratio of around 3.5 at a temperature range of 250-300°C and an M/P ratio of 1.9 was obtained by Collins et al [44]. Studying M/P ratio, two opposite phenomena affecting this ratio have to be noticed. P-xylene has a large advantage over m-xylene due to it is high diffusion rate. However, m-xylene has a great advantage because it can easily be formed via 1,2 methyl shift. Due to these contradictory phenomena, a reasonable M/P ratio was obtained. Huge value of M/P was reported over USY [48]. M/P ratios of around 9, 6 and 4 for 400, 450, and 500°C respectively were measured [48]. The large M/P ratio over USY is expected since the advantage of p-xylene in USY no longer exists.

4.2.2 Xylene Disproportionation (D)

Disproportionation reaction requires two molecules of xylene reactants with bulky transition state intermediates. As a result, disproportionation is significant on large pore zeolites that can accommodate these intermediates. However, in ZSM-5 zeolites with a smaller pore size, it is difficult to form the intermediates of disproportionation pathway (restricted transition state selectivity). Therefore, xylene transformation over ZSM-5 zeolite is generally considered to favor the unimolecular isomerization pathway.

Fig 5a shows that disproportionation over ZSM-5 based catalyst is a primary reaction and all isomers undergo similar disproportionation reaction rate at 400°C. However, as temperature increases to 500°C, m-xylene starts to have an advantage in disproportionation selectivity over the other xylene isomers as shown in Fig 5b. For all isomers, disproportionation is primary reaction as shown in Figs 5a and 5b.

It is significant to mention that generally ZSM-5 is more selective to isomerization reaction than disproportionation reaction. For example, at 400°C and 20 % xylene conversion, Fig 3a shows that isomerization yield is 12.5 wt% and from Fig 5a the disproportionation yield at same temperature and conversion is about 7 wt%. Therefore, at 400°C the isomerzation selectivity is 62.5 % and the disproportionation selectivity is 35%. Furthermore, it was found that the isomerization selectivity decreased to 57% and disproportionation selectivity increased to 40% by increasing reaction temperature to 500°C (see Figs 3b and 5b). At similar conversion, Iliyas and Al-Khattaf [48] found that disproportionation selectivity is higher than isomerization selectivity for m-xylene conversion over USY zeolite.

4.6 Modeling Results

The intrinsic kinetic parameters for each isomer (*ko, E, & α*) were determined using non linear regression of the experimental data and are reported in Tables 5-10 with their corresponding 95% confidence limits and matrix correlations. The correlation matrices displayed low cross-correlation between the regressed parameters indicating accurate fit. The results in Tables 5,7 and 9 show that the intrinsic activation energy for the m- & o-xylene reactions (E_R) are generally equal and double that for p-xylene reactions. Choudhary and Akolekar [28] reported activation energy of 9-11 kcal/mol for o-xylene transformation which is in great agreement with 10 kcal/mol obtained by the present study.

Effectiveness Factor η_{ss}

The effectiveness factor of the transformation of the three xylene isomers was calculated based on equation 5. In order to evaluate η_{ss}, modified Thiele modulus, h', has to be calculated. Equation 6 can be used to find h'. The modified Thiele modulus was calculated based on two different diffusivities. The first value of xylene diffusivities were

taken from Choudhary et al, [34] and the second set of xylene diffusivities were calculated based on Han et al [33] results and $D_P=100D_O=1000D_M$ ratios.

Tables 11-13 report h'.and η_{ss} for p-xylene, o-xylene and m-xylene respectively. These values are calculated based on Choudhary et al [34], diffusivities. It can be noticed that m-xylene effectiveness factor is very low at all conditions indicating a high diffusion limitation for m-xylene reaction inside ZSM-5 zeolite. O-xylene, on the other hand, shows middle range effectiveness factor in a range of 0.55 - 0.66. It can be observed that $\boldsymbol{\eta_{ss}}$ increases with both conversion and reaction temperature. These results are consistent with that observed by Ma and Savage [14] who reported a 0.5 effectiveness factor for o-xylene reaction over ZSM-5 at 523K.

The major problem in using Choudhary et al [34] data in the kinetic equation was noticed with p-xylene equation. It can be seen from Tables 12 and 13 that $\boldsymbol{\eta_{ss}}$ for p-xylene is similar to that for o-xylene (0.55-0.66 range). However, these $\boldsymbol{\eta_{ss}}$ values are not consistent with both our experimental data which showed p-xylene conversion is higher than that of o-xylene. Furthermore, accordance to the literature, the diffusivity of p-xylene should be clearly higher than that of o-xylene. Calculating the diffusivities of p-xylene and o-xylene at 400°C and 500°C using Choudhary et al [34] parameters which are shown in Table 1b, indicates that Choudhary et al [34] parameters for p-xylene diffusivity can not be used for high temperature. For example, Table 1b reports a diffusivity of $2.4\text{x}10^{-14}$ m^2/sec for o-xylene at 400°C. Garcia and Weisz [21] found o-xylene diffusivity at 400°C over ZSM-5 to be $2\ \text{x}10^{-14}$ m^2/sec which is in excellent agreement with that found by Choudhary et al [31]. Moreover, o-xylene $\boldsymbol{\eta_{ss}}$ calculated in the present study is in the same level as that found by Ma and Savage [14]. Furthermore, at 315°C and over ZSM-5 Bhatia [49] reported diffusivity of 10^{-14} m^2/sec and 10^{-11} m^2/sec for o-xylene and p-xylene respectively. Therefore, the diffusivity parameters for p-xylene are too low and the confident is much more with o-xylene parameters. Consequently, the p-xylene diffusivity parameters measured are too low to be used at high temperature.

Han et al [33] studied the intracrystalline diffusivity of p-xylene (gas phase) in ZSM-5 at higher temperature range than Choudhary et al [34]. Their temperature range was 100°C - 200°C. The diffusion parameters calculated based on their data are listed in Table 1a. Regarding o-xylene and m-xylene diffusivities, they are calculated based on p-xylene

diffusivity. Since $D_P = 100D_O = 1000D_M$, knowing D_P, the other diffusivities can be evaluated.

Tables 11-13 report h' **.and** η_{ss} for p-xylene, o-xylene and m-xylene respectively. These values were calculated based on Han et al [33], diffusivities. It can be depicted from these tables that m-xylene η_{ss} are < 0.1 for all reaction conditions. Therefore, it can be concluded that m-xylene molecules encounter considerable diffusion obstacle when they react inside ZSM-5 zeolite. This also explains the lowest conversion obtained by m-xylene compared to the other xylene isomers in all reaction conditions as shown in Figs 2a and 2b.

O-xylene η_{ss} seems to be in a middle range between 0.3-0.5 smaller than that obtained based on Choudhary et al [34] data. It is important to mention that Olson and Haag [24] calculated η_{ss} of o-xylene reaction over ZSM-5 at 482°C to be 0.05, however, they used very low o-xylene diffusivity of $5x10^{-16}$ m^2/sec. P-xylene has a close to unity η_{ss} indicating that p-xylene reaction inside ZSM-5 is free from any mass transport barrier. Both o-xylene and p-xylene η_{ss} are in great consistency with the experimental results shown in both Figs 2a and 2b. Finally, Figs 6a and 6b show the plot of effectiveness factor versus modified Thiele modulus at 400°C and 500°C respectively. In both figures, it can be seen that m-xylene suffers from extreme diffusion barrier followed by o-xylene with a reasonable diffusion limitation followed by p-xylene with almost no diffusion limitation inside ZSM-5 structure.

To check the validity of the estimated kinetic parameters using with the overall kinetic model for the three isomers, the fitted parameters were substituted into the model equations, and the equations were solved numerically using the fourth order Runge-Kutta method. The simulated results were compared with the experimental data as shown in Figures 7a-7c for m-xylene, o-xylene and p-xylene conversions respectively. It can be observed from these figures that the simulated results compare fairly well with the experimental data. This provides significant evidence that the overall model could be used for the interpretation of the data obtained during m-xylene transformation in the riser simulator.

In summary, the good agreement between the model and experimental results proves that the reaction-diffusion model can be used to successfully model the overall xylene transformation.

Conclusions

The following conclusions can be drawn from transformations of the three xylene isomers over ZSM-5 in the riser simulator under the conditions of the present study:

1. The reactivity of the xylene isomers was found to decrease in the sequence: p-xylene > o-xylene > m-xylene. This was attributed to the difference in the diffusion and adsorption capacities of the xylenes, which favors the isomers in the above sequence.

2. At low temperature (400°C) all xylene isomers react in similar way. Therefore, isomerization and disproportionation yields are identical at the same conversion. However, at higher temperature, m-xylene was shown to have lowest isomerization yield and highest disproportionation yield compared to the other xylene isomers. P-xylene and o-Xylene, on the other hand, have similar isomerization and disproportionation yields.

3. P/O ratio was found to be higher than thermodynamic value and decreases with temperature. The decrease in P/O ratio with temperature during m-xylene transformation suggests that p-xylene selectivity is favored at lower than at higher temperature.

4. Similar to P/O ratio, M/O was found to be higher than thermodynamic value and decreases with temperature. The higher value of M/O ratio than the equilibrium value, particularly in the initial stage of the reaction, confirms that p-xylene isomerization proceeds via 1,2-methyl shifts with ZSM-5 and 1,3 methyl shifts becomes more significant at higher reaction temperature.

5. Isomerization reaction was found to advance at a higher rate than disproportionation during the conversion of the three xylene isomers over ZSM-5.

6. The kinetics of vapor-phase transformation of xylenes has been carried out over ZSM-5 zeolite catalyst using the riser simulator. Kinetic models which consider the different diffusivities of the three xylene isomers have been developed.

7- The effectiveness factors of m-xylene, o-xylene and p-xylene reactions over ZSM-5 have been calculated. Results show the p-xylene reaction has the highest effectiveness factor (almost unity) followed by o-xylene, m-xylene was found to have the lowest effectiveness factor. These results are in great consistency with the experimental data.

Acknowledgment

The authors gratefully acknowledge King Fahd University of Petroleum & Minerals for the financial support provided for this work. I would like also to thank Mr. Mariano Gica for his useful collaboration on the experimental work.

Nomenclature

C_A reactant concentration in the riser simulator (mole/m^3)

CFL confidence limit

E_R energy of activation due to reaction, kcal/mol

E_D energy of activation due to diffusion, kcal/mol

$k_{A,in}$ Intrinsic kinetic rate constant (m^3/kgcat.sec)

$= k'_0 exp[\frac{-E_R}{R}(\frac{1}{T} - \frac{1}{T_0})$

$k_o^{'}$ Pre-exponential factor in Arrhenius equation defined at an average temperature [m^3/kgcat.sec], units based on first order reaction

D_o Diffusion coefficient constant, m^2/s

D_{eff} Effective Diffusion coefficient, m^2/s

$h^{'}$ $\frac{1}{a_{ext}}\sqrt{\frac{k_{A,in}\rho_{cr}\varphi_{in}}{D_{eff}}}$; Modified Thiele Modulus

η_{ss} $\frac{\tanh(h^{'})}{h^{'}}$; Effectiveness factor

ρ_{cr} Density of zeolite crystal, kg/m^3

r correlation coefficient

R universal gas constant, kcal/kmol K

t reaction time (sec).

T reaction temperature, K

To average temperature of the experiment, K

V volume of the riser (45 cm^3)

W_{cr} mass of the catalysts (0.81 gcat)

y_A reactant mass fraction (wt%)

Greek letters

α Deactivation constant, s^{-1} (TOS Model)

φ Deactivation function, dimensionless

References

(1) Lanewala, M. A.; Bolton, A. P. *J. Org. Chem.* **1969**, 34(10), 3107-12.

(2) Cortes, A.; Corma, A. *J. Catal.* **1978**, 51(3), 338-44.

(3) Corma, A.; Sastre, E. *J. Catal.* **1991**, 129(1), 177-85.

(4) Morin, S.; Gnep, N. S.; Guisnet, M. *J. Catal.* **1996**, 159(2), 296-304

(5) Al-Khattaf, S.; Tukur, N. M.; Al-Amer, A. *Ind. & Eng. Chem. Res.* **2005**, 44(21), 7957-7968

(6) Jones, Christopher W.; Zones, Stacey I.; Davis, Mark E. *Appl. Catal., A: Gen.* **1999**, 181(2), 289-303.

(7) Zheng, S.; Jentys, A.; Lercher, J. A. *J. Catal*. **2006**, 241, 304-311.

(8) Llopis, F. J; Satre, G; Corma, A. *J. Catal*. **2006**, 242, 195-206.

(9) Chen, N. Y.; Kaeding, W. W.; Dwyer, F. G. *J. Amer. Chem. Soc.* **1979**, 101(22), 6783-4.

(10) Kaeding, W. W.; Chu, C.; Young, L. B.; Weinstein, B.; Butter, S. A. *J. Catal.* **1981**, 67(1), 159-74.

(11) Kaeding, W. W.; Chu, C.; Young, L. B.; Butter, S. A. *J. Catal.* **1981**, 69(2), 392-8.

(12) Young, L. B.; Butter, S. A.; Kaeding, W. W. *J. Catal*. **1982**, 76(2), 418-32.

(13) Chang, Xiaodong; Li, Yuguang; Zeng, Zhaohuai. *Ind. & Eng. Chem. Res.* **1992**, 31(1), 187-92.

(14) Ma, Y. H.; Savage, L. A *AIChE J.* **1987**, 33(8), 1233-40.

(15) Nayak, V. S.; Riekert, L. *Appl. Catal.* **1986**, 23(2), 403-11.

(16) Kuerschner, U.; Parlitz, B.; Schreier, E.; Oehlmann, G.; Voelter, J. *Appl. Catal.* **1987**, 30(1), 159-66.

(17) Vinek, H.; Lercher, J. A. *J. Mol. Catal.* **1991**, 64(1), 23-39.

(18) Vedrine, J. C.; Auroux, A.; Dejaifve, P.; Ducarme, V.; Hoser, H.; Zhou, S. *J. Catal.* **1982**, 73(1), 147-60.

(19) Tsai, Tseng-Chang; Liu, Shang-Bin; Wang, I. *Appl. Catal., A: Gen.* **1999**, 181(2), 355-398.

(20) Weisz, P. B.; Frilette, V. J. *J. Phys. Chem.* **1960**, 64, 382-3.

(21) Garcia, Sigfrido F.; Weisz, Paul B. *J. Catal.* **1993**, 142(2), 691-6.

(22) Wei, J. *J. Catal.* **1982**, 76(2), 433-9.

(23) Cejka, J.; Wichterlova, B. *Cat. Rev*. **2002**, 44(3), 375-421.

(24) Olson, D. H.; Haag, W. O. *ACS Symposium Series, (Catal. Mater.: Relat. Struct. React.)*, **1984,** 248, 275-307.

(25) Werner, O, Haag, W. O., Lago, R.M., Weisz, P.B., Faraday Disc.,**1982**, 72, 317.

(26) Chutoransky, P., Jr.; Dwyer, F. G. *Adv. Chem. Ser. (Mol. Sieves, Int. Conf., 3rd)*. **1973**, 121, 540-52.

(27) Chen, N. Y.; Kaeding, W. W.; Dwyer, F. G. *J. Amer. Chem. Soc.* **1979**, 101(22), 6783-4.

(28) Choudhary, Vasant R.; Akolekar, Deepak B. *J. Catal.* **1989**, 116(1), 130-43.

(29) Al-Khattaf, S.; Atias, J. A.; Jarosch, K.; de Lasa, H. *Chem. Eng. Sci.* **2002**, 57(22-23), 4909-4920.

(30) Al-Khattaf, S.; Tukur, N. M.; Al-Amer, A.; Al-Mubaiyedh, U. A. *Appl. Catal., A: Gen.* **2006**, 305(1), 21-31.

(31) Hedlund, J.; Oehrman, O.; Msimang, V.; van Steen, E.; Boehringer, W.; Sibya, S.; Moeller, K. *Chem. Eng. Sci.* **2004**, 59(13), 2647-2657.

(32) Mirth, G.; Cejka, J.; Lercher, J. A. *J. Catal.* **1993**, 139(1), 24-33.

(33) Han, Minghan; Yin, Xiuyan; Jin, Yong; Chen, Shu. *Ind. & Eng. Chem. Res.* **1999**, 38(8), 3172-3175.

(34) Choudhary, Vasant R.; Nayak, Vikram S.; Choudhary, Tushar V. *Ind. & Eng. Chem. Res.* **1997**, 36(5), 1812-1818.

(35) de Lasa, H. T., *US Patent* 5 **1992**, 102, 628.

(36) Al-Khattaf, S.; de Lasa, H. *Ind. & Eng. Chem. Res.* **2001**, 40(23), 5398-5404.

(37) Al-Khattaf, S.; de Lasa, H. *Appl. Catal., A: Gen.* **2002**, 226(1-2), 139-153.

(38) Kraemer, D. W., *Ph.D. Dissertation*, University of Western Ont., London, Canada **1991**.

(39) Voorhies, Alexis, Jr. *J. Ind. Eng. Chem.* **1945**, 37, 318-22.

(40) Choudhary, V. R.; Akolekar, D. B. *J. Mol. Catal.* **1990**, 60(2), 173-88.

(41) Chen , N. Y. *J. Catal.* **1982**, 114, 17.

(42) 40- Roque-Malherbe, R.; Ivanov, V. *Microp. Mesop. Mater.* **2001**, 47(1), 25-38.

(43) Armaroli, T.; Bevilacqua, M.; Trombetta, M.; Alejandre, A. G.; Ramirez, J.; Busca, G. *Appl. Catal, A: Gen.* **2001**, 220(1-2), 181-190.

(44) Collins, Dermot J.; Medina, Roger J.; Davis, Burtron H. *Can J. Chem. Eng.* **1983**, 61(1), 29-35.

(45) Hsu, Y. S.; Lee, T. Y.; Hu, H. C. *Ind. & Eng. Chem. Res.* **1988**, 27(6), 942-7.

(46) Martens, J. A.; Perez-Pariente, J.; Sastre, E.; Corma, A.; Jacobs, P. A. *Appl. Catal.*

(47) Mirth, G.; Cejka, J.; Nusterer, E.;Lercher, J. A. *Stud. Surf. Sci. Catal.* **1994**, 83, 287. **1988**, 45(1), 85-101.

(48) Iliyas, A.; Al-Khattaf, S. *Appl. Catal., A: Gen.* **2004**, 269(1-2), 225-236.

(49) Bhatia, S. *Zeolite catalysis, principle and applications*, Vol. 7-18 (pp. 69). Boca Raton: CRC Press, **1990**.

Table 1a: Diffusion Coefficient parameters over ZSM-5

Source	*m*-xylene		*o*-xylene		*p*-xylene	
	Do (m^2/s)	E (Kcal/mol)	Do (m^2/s)	E (Kcal/mol)	Do (m^2/s)	E (Kcal/mol)
Choudhary et al. [34]	$5.8x10^{-13}$	9.0	$9.1x10^{-12}$	8.5	$6.2x10^{-13}$	4.3
Han et al. [33]	*		*		$4.87x10^{-12}$	1.85

*Diffusion coefficients for the *m*- & *o*- xylene isomers are taken to be ($p : o: m \approx 1000 : 10 : 1$) in accordance with Mirth et al. [32].

Table 1b: Diffusivities Coefficients of o-xylene and p-xylene over ZSM-5 calculated based on Choudhary et al. [34]

Component	Diffusivity (m^2/sec) At 400°C	Diffusivity (m^2/sec) At 500°C
o-xylene	$2.4x10^{-14}$	$3.6x10^{-14}$
p-xylene	$1.6x10^{-14}$	$3.7x10^{-14}$

Table 2: Product distribution (wt %) at various reaction conditions for *m*-xylene transformation.

Temp (^{o}C)/ time (s)	Conv. (%)	*p*-xylene	*o*-xylene	Toluene	*1,3,5-* TMB	*1,2,4-* TMB	*1,2,3-* TMB	TeMBs
400								
3	4.9	1.6	1.1	1.0	0.3	0.73	0.09	0
5	8.8	3.1	1.9	1.7	0.5	1.2	0.2	0.1
7	10.1	3.8	2.2	1.9	0.6	1.5	0.2	0.1
10	12.3	4.9	2.7	2.2	0.7	1.6	0.2	0.1
13	16.3	5.6	3.48	3.2	1.0	2.4	0.3	0.2
15	21	7	4	3.7	1.0	2.8	0.4	0.2
450								
3	7.8	2.3	1.7	1.7	0.5	1.3	0.2	0.1
5	10	2.7	2.1	2.4	0.6	1.6	0.25	0.2
7	13.0	3.5	2.6	2.8	0.8	2.0	0.3	0.25
10	21.0	6.7	4.4	4.0	1.1	2.8	0.4	0.25
13	25.0	7.7	5.3	5.3	1.4	3.8	0.6	0.4
15	26.6	8.4	5.6	6.1	1.6	4.2	0.6	0.45
500								
3	9	2.5	2	2.1	0.6	1.4	0.2	0.2
5	12	2.6	2.3	3.1	0.8	2.1	0.3	0.35
7	18	4.8	3.6	4.5	1.1	2.8	0.5	0.4
10	24.0	6.2	5	5.7	1.4	4.0	0.6	0.6
13	28.1	7.2	5.9	6.8	1.7	4.8	0.7	0.7
15	30.8	8.2	6.3	7.3	1.8	5	0.8	0.8

Table 3: Product distribution (wt %) at various reaction conditions p-xylene transformation.

Temp (°C)/ time (s)	Conv. (%)	*m*-xylene	*o*-xylene	Toluene	*1,3,5-* TMB	*1,2,4-* TMB	*1,2,3-* TMB	TeMBs
400								
3	7	3	1.0	1.5	0.3	0.9	0.1	0.1
5	11	4.8	1.4	2.2	0.4	1.5	0.2	0.25
7	16.1	7.1	2.0	3.3	0.6	2.3	0.25	0.3
10	21.7	10.6	2.8	4.0	0.7	2.7	0.3	0.4
13	25.8	12.2	3.4	4.8	1.0	3.3	0.4	0.5
15	32	15.4	4.2	6	1.1	4	0.5	0.6
450								
3	9.3	4	1.3	2	0.4	1.3	0.2	0.2
5	16.4	7.6	2.2	3.2	0.6	2.1	0.3	0.3
7	21	9.6	2.8	4	0.9	2.7	0.4	0.45
10	27	12.7	3.7	5.2	1.1	3.4	0.5	0.55
13	33	15.5	4.6	6.2	1.4	4.2	0.6	0.7
15	38.3	17.6	5.3	7	1.6	4.6	0.6	0.75
500								
3	12	5	1.7	2.5	0.6	1.6	0.25	0.25
5	19	7.8	2.7	4	0.9	2.5	0.4	0.5
7	24.3	10.2	3.4	5	1.1	3.2	0.5	0.6
10	32.3	13.4	4.7	6.7	1.4	4.2	0.7	0.7
13	37.5	16	5.5	7.6	1.6	4.8	0.75	0.8
15	42.5	18	6.3	8.6	2	5.5	0.8	0.9

Table 4: Product distribution (wt %) at various reaction conditions for o-xylene transformation.

Temp (^{o}C)/ time (s)	Conv. (%)	*p*-xylene	*m*-xylene	Toluene	*1,3,5-* TMB	*1,2,4-* TMB	*1,2,3-* MB	TeMBs
400								
3	6	1.1	2.5	1.0	0.22	0.9	0.13	0
5	9.2	1.9	4.2	1.4	0.3	1.1	0.2	0
7	10.5	2.0	4.3	1.8	0.44	1.5	0.2	0
10	15	3.2	6.8	2.1	0.5	1.9	0.3	0
13	17.3	3.7	7.7	2.6	0.6	2.3	0.35	0.1
15	22.3	5	10	3.2	0.7	2.6	0.4	0.12
450								
3	8.4	1.4	3.2	1.6	0.4	1.3	0.2	0.1
5	11.4	2.2	4.8	1.9	0.43	1.6	0.25	0.1
7	14.6	2.8	6.2	2.4	0.6	2.0	0.3	0.12
10	21	4.1	9.1	3.5	0.85	2.7	0.4	0.14
13	23.5	4.8	10	3.8	0.9	3.1	0.5	0.2
15	31.3	6.1	13.4	5.2	1.2	4.0	0.65	0.35
500								
3	10	1.7	3.9	1.9	0.5	1.4	0.2	0.15
5	14.3	2.3	5.1	3.0	0.7	2.1	0.3	0.3
7	21.3	3.7	8.4	4.0	1.0	3.0	0.5	0.35
10	28.3	4.8	10.8	5.6	1.4	4.0	0.7	0.5
13	34.1	6	13.2	6.5	1.6	4.9	0.8	0.6
15	37.5	6.6	14.4	7.4	1.8	5.3	0.8	0.7

Table 5: Kinetic constants for *m*-xylene transformation [Basis for Diffusion data - Hans et al.[33]]

k_0' (m^3/kg-cat.sec)	95% CFL	E_R (kcal/mol)	95% CFL	α (1/sec)	95% CFL	r^2
23.56E-03	4.87E-03	10.32	1.49	0.02	0.03	0.99

Table 6: Correlation matrix (*m*-xylene)

k_0'	1	-0.29	0.93
E_R	-0.29	1	-0.03
α	0.93	-0.03	1

Table 7: Kinetic constants for *o*-xylene transformation [Basis for Diffusion data - Hans et al.[33]]

k_0' (m^3/kg-cat.sec)	95% CFL	E_R (kcal/mol)	95% CFL	α (1/sec)	95% CFL	r^2
3.61E-03	0.65E-03	9.97	1.30	0.03	0.03	0.99

Table 8: Correlation matrix for (*o*-xylene)

k_0'	1	-0.28	0.93
E_R	-0.28	1	-0.05
α	0.93	-0.05	1

Table 9: Kinetic constants for *p*-xylene transformation [Diffusion data from Hans et al.[33]]

$k_0^{'}$ (m^3/kg-cat.sec)	95% CFL	E_R (kcal/mol)	95% CFL	α (1/sec)	95% CFL	r^2
1.92E-03	0.15E-03	4.74	0.58	0.02	0.01	0.99

Table 10: Correlation matrix (*p*-xylene)

$k_0^{'}$	1	-0.27	0.93
E_R	-0.27	1	-0.04
α	0.93	-0.04	1

Table 11: Effectiveness factor and Thiele Modulus for *m*-xylene (crystal size (L) = 1.0 μm)

Temperature (oC)/Time (s)	Conversion (%)	h′	η	h′	η
		Diffusion data from Choudhary et al.[34]		Basis for Diffusion data - Hans et al.[33]	
400					
3	5	28.86	0.0346	17.748	0.0563
5	8	28.80	0.0347	17.397	0.0575
7	10	28.73	0.0348	17.052	0.0586
10	14	28.62	0.0349	16.548	0.0604
13	17	28.52	0.0351	16.059	0.0623
15	19.5	28.45	0.0351	15.741	0.0635
450					
3	7	25.14	0.0398	22.091	0.0453
5	10	25.08	0.0399	21.653	0.0462
7	12	25.02	0.0400	21.225	0.0471
10	20	24.93	0.0401	20.597	0.0485
13	24	24.84	0.0403	19.989	0.0500
15	26.5	24.78	0.0404	19.593	0.0510
500					
3	9	22.29	0.0449	26.729	0.0374
5	12	22.23	0.0450	26.200	0.0382
7	18.5	22.18	0.0451	25.681	0.0389
10	24	22.10	0.0452	24.922	0.0401
13	28	22.02	0.0454	24.185	0.0413
15	33	21.97	0.0455	23.706	0.0422

Table 12: Effectiveness factor and Thiele Modulus for *o*-xylene (L = 1.0 μm)

Temperature (oC)/Time (s)	Conversion (%)	h′	η	h′	η
		Diffusion data from Choudhary et al.[34]		Basis for Diffusion data - Hans et al.[33]	
400					
3	6	1.678	0.5559	2.178	0.4474
5	9	1.643	0.5648	2.116	0.4591
7	12	1.609	0.5737	2.055	0.4709
10	15.5	1.559	0.5871	1.967	0.4888
13	19	1.510	0.6005	1.883	0.5069
15	23.5	1.479	0.6094	1.829	0.5192
450					
3	8.5	1.564	0.5857	2.687	0.3687
5	12	1.532	0.5946	2.610	0.3790
7	16	1.500	0.6035	2.535	0.3895
10	21	1.453	0.6168	2.427	0.4057
13	25	1.408	0.6299	2.323	0.4223
15	31.3	1.379	0.6387	2.257	0.4335
500					
3	10	1.472	0.6115	3.226	0.3090
5	14	1.441	0.6203	3.133	0.3180
7	21	1.411	0.6291	3.043	0.3271
10	28	1.367	0.6422	2.913	0.3412
13	34	1.325	0.6551	2.789	0.3559
15	38	1.297	0.6637	2.709	0.3659

Table 13: Effectiveness factor and Thiele Modulus for *p*-xylene (L = 1.0 μm)

Temperature (oC)/Time (s)	Conversion (%)	h′	η	h′	η
		Diffusion data from Choudhary et al.[34]		Diffusion data from Hans et al.[33]	
400					
3	7	1.648	0.5634	0.173	0.9901
5	10.5	1.588	0.5794	0.170	0.9904
7	16	1.529	0.5952	0.167	0.9908
10	22	1.446	0.6189	0.163	0.9912
13	26	1.367	0.6423	0.159	0.9917
15	32	1.317	0.6576	0.156	0.9920
450					
3	9.5	1.643	0.5648	0.187	0.9885
5	16	1.583	0.5807	0.184	0.9889
7	21	1.524	0.5966	0.180	0.9893
10	27	1.441	0.6203	0.176	0.9898
13	33	1.363	0.6436	0.171	0.9904
15	38	1.313	0.6589	0.168	0.9907
500					
3	12	1.638	0.5660	0.199	0.9870
5	19	1.578	0.5819	0.196	0.9874
7	24.2	1.520	0.5978	0.192	0.9878
10	32.5	1.437	0.6214	0.187	0.9885
13	38	1.359	0.6447	0.183	0.9890
15	43.5	1.309	0.6601	0.179	0.9894

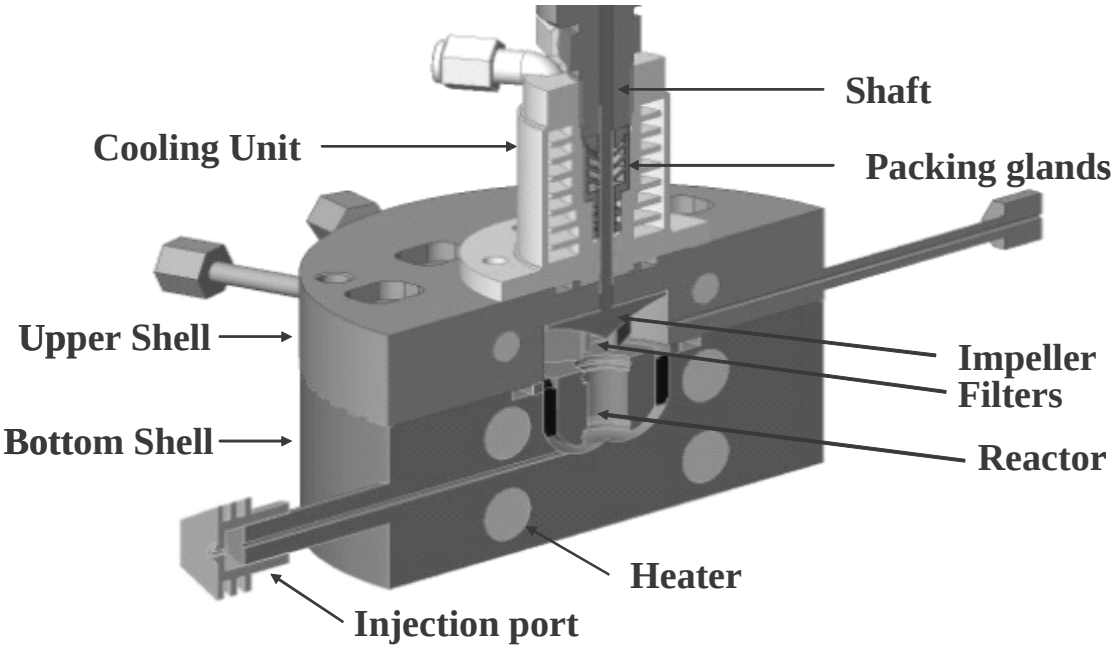

Fig. 1. Schematic diagram of the riser simulator

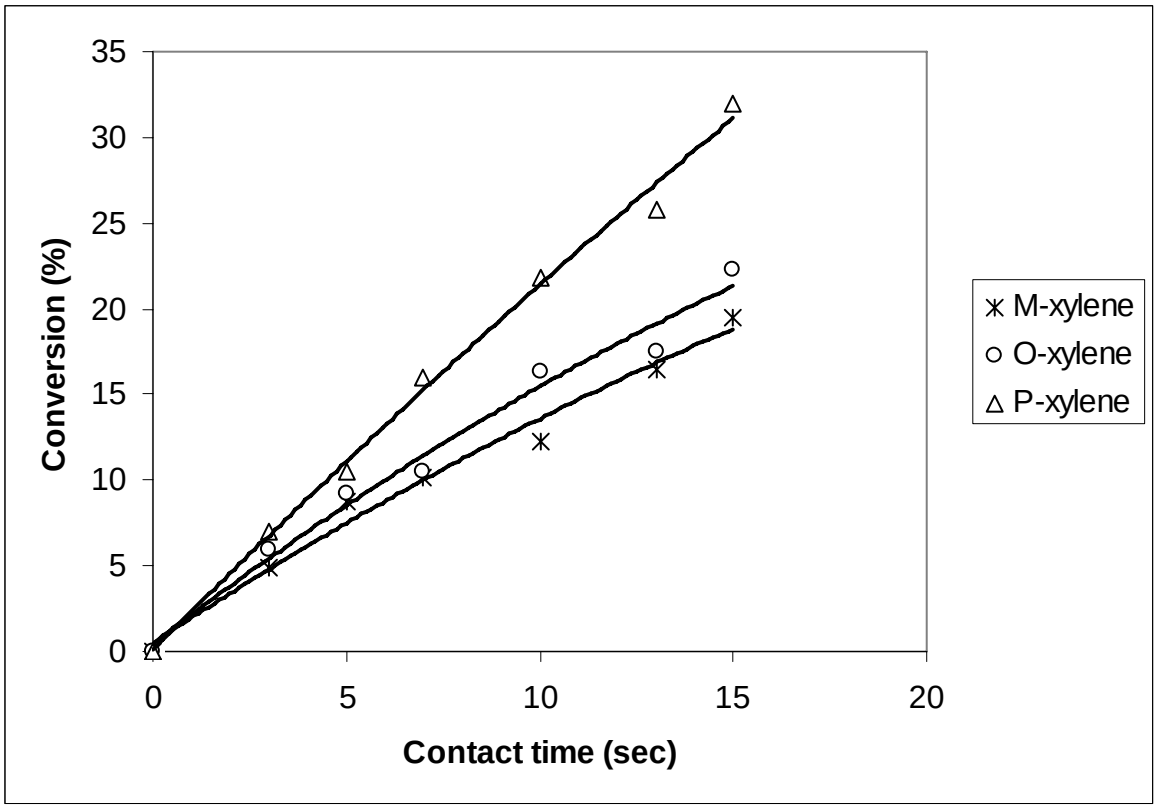

Fig 2a. Xylenes conversion versus contact time at 400°C.

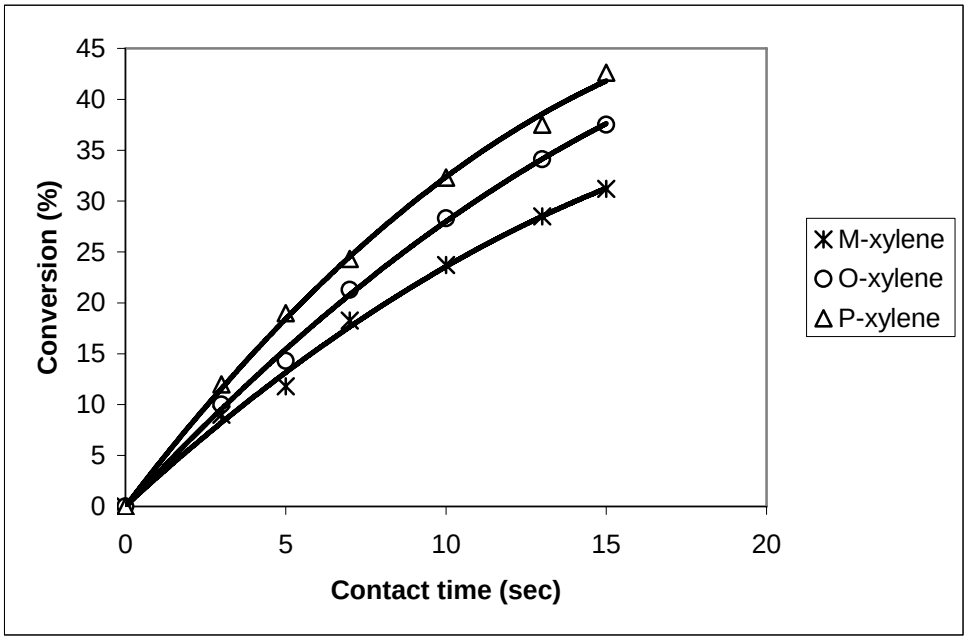

Fig 2b. Xylenes conversion versus contact time at 500°C.

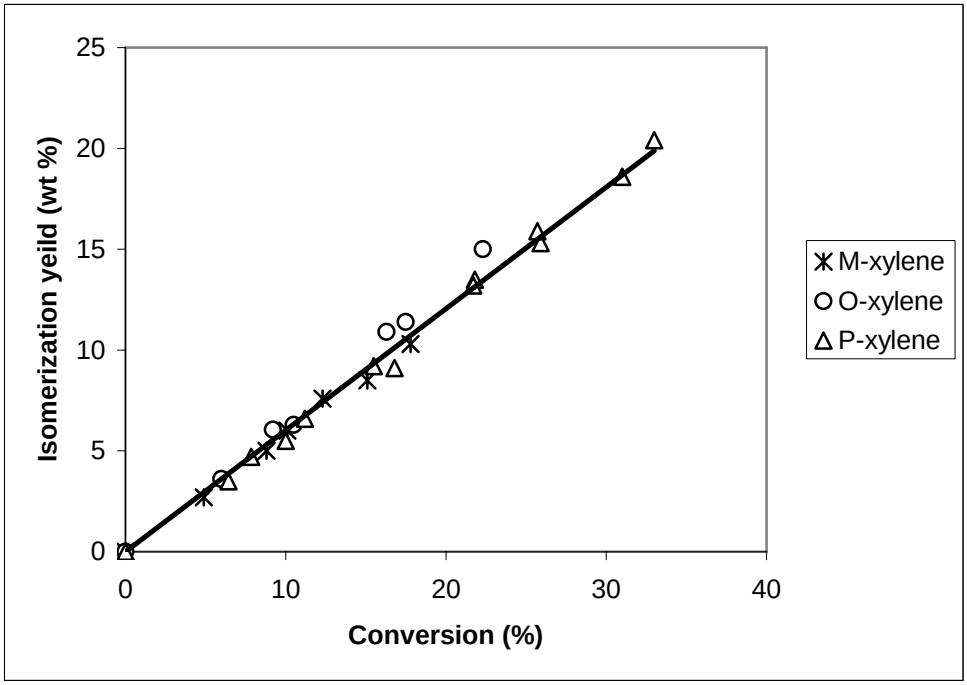

Fig 3a Isomerization yield versus xylene conversion at 400°C.

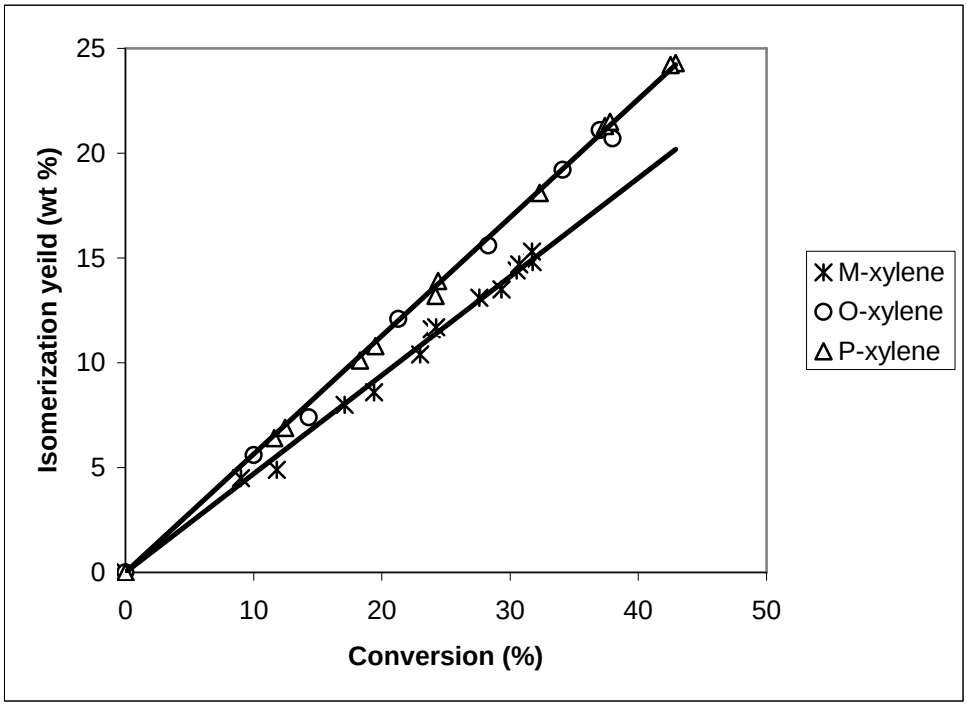

Fig 3b. Isomerization yield versus xylene conversion at 500°C.

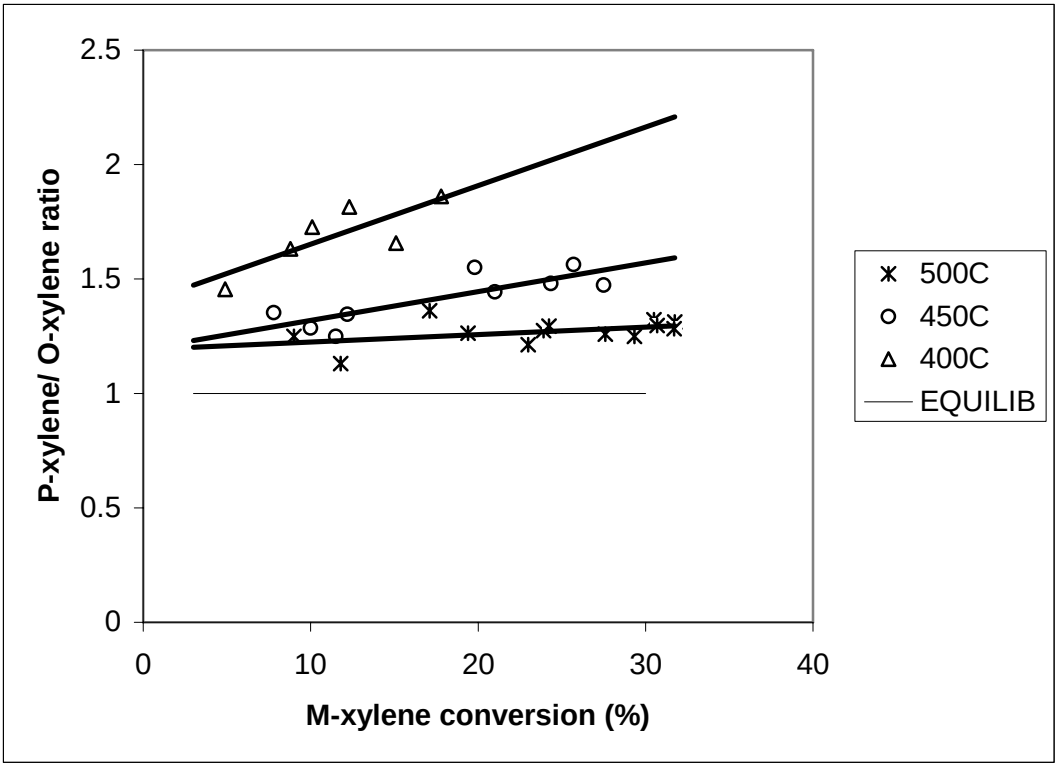

Fig 4a. P/O ratio as function of m-xylene conversion at different temperatures.

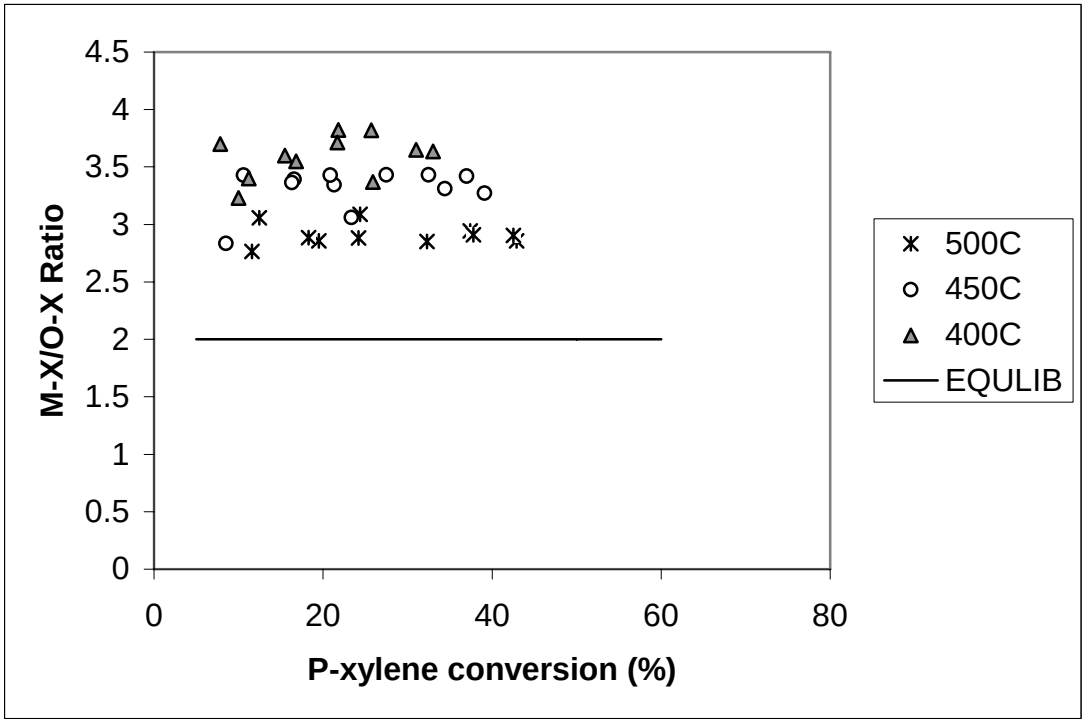

Fig 4b. M/O ratio as function of p-xylene conversion at different temperatures.

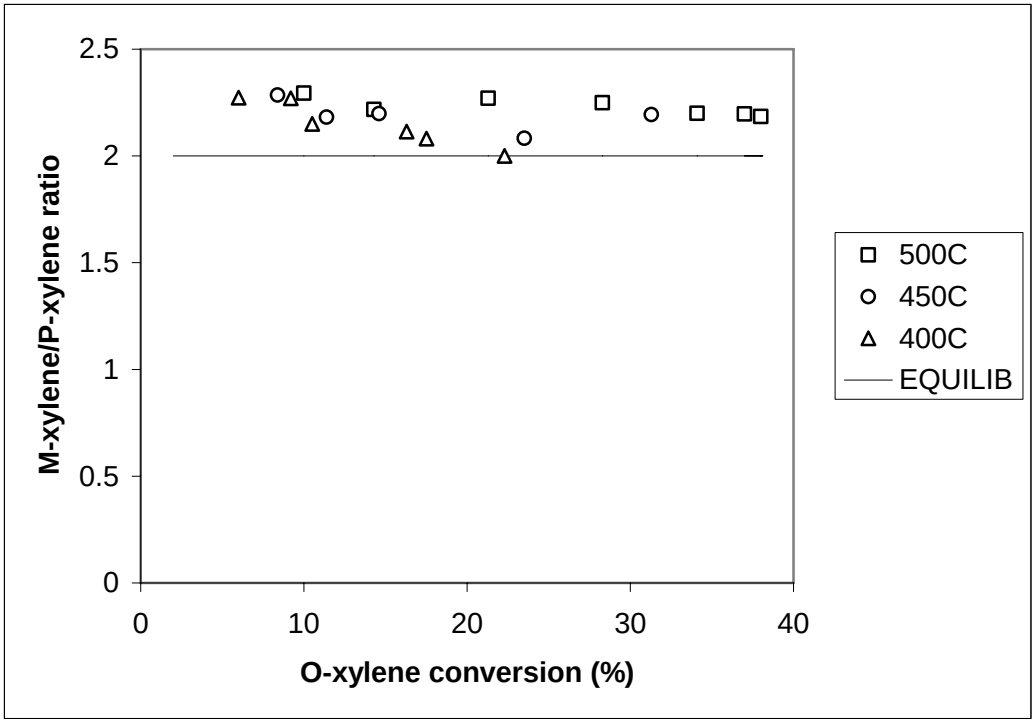

Fig 4c. M/P ratio as function of o-xylene conversion at different temperatures.

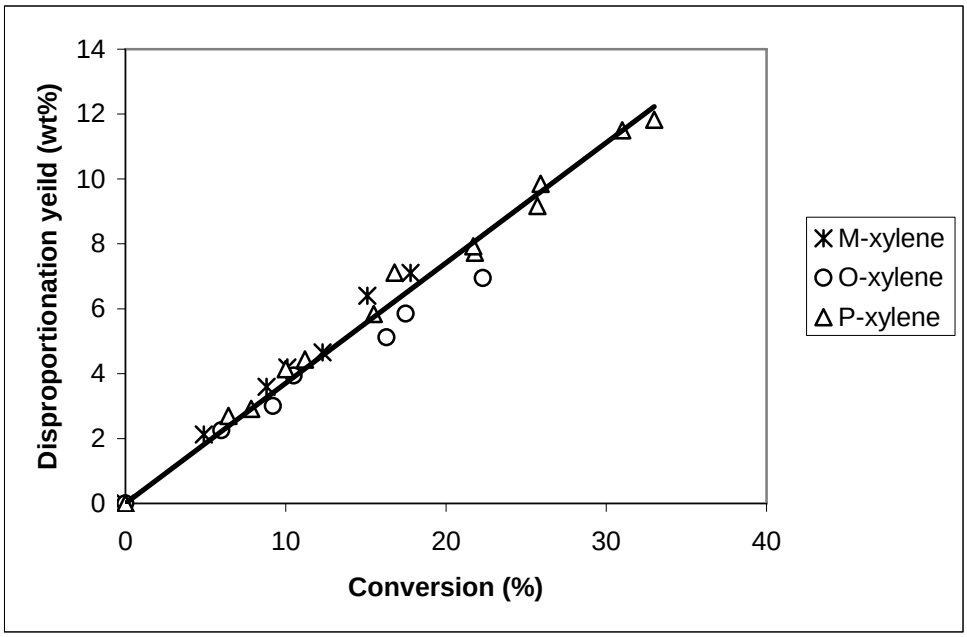

Fig 5a. Disproportionation yield versus xylene conversion at 400°C.

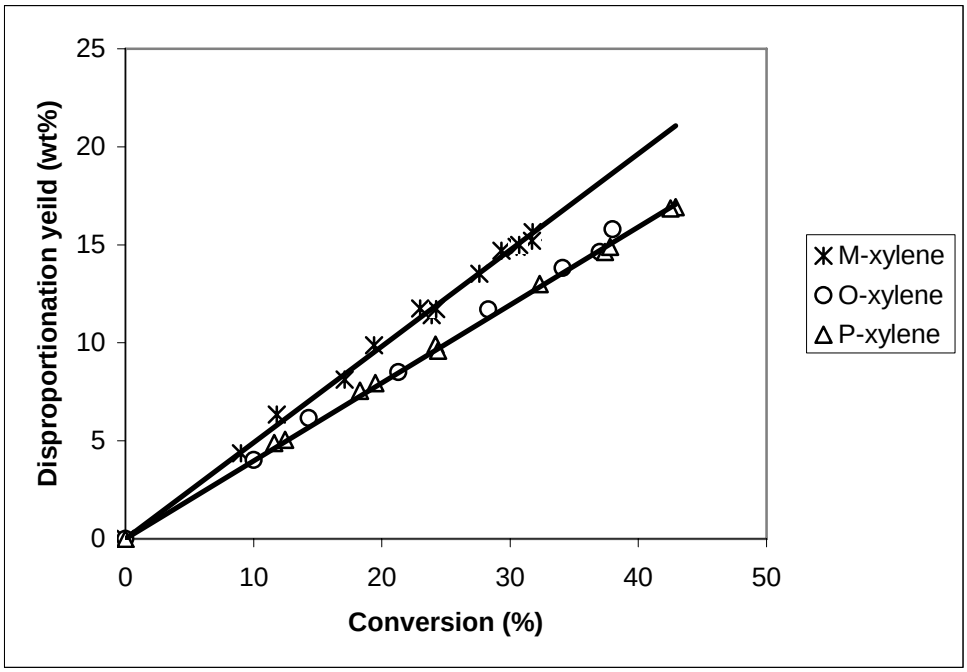

Fig 5b. Disproportionation yield versus xylene conversion at 500°C

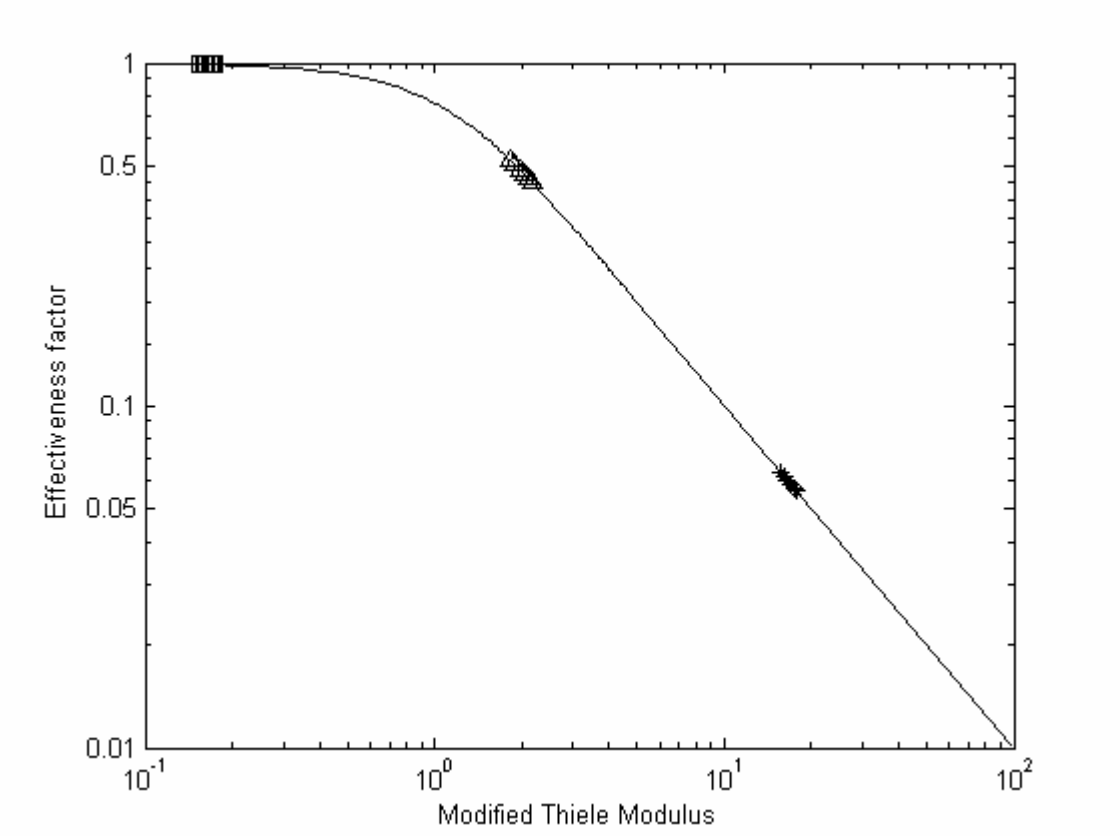

Figure 6a: Effectiveness factor versus modified Thiele Modulus. $T = 400^{o}C$, (*) *m*-xylene, (Δ) *o*-xylene, and (□) *p*-xylene [Basis for Diffusion data - Hans et al.[33]].

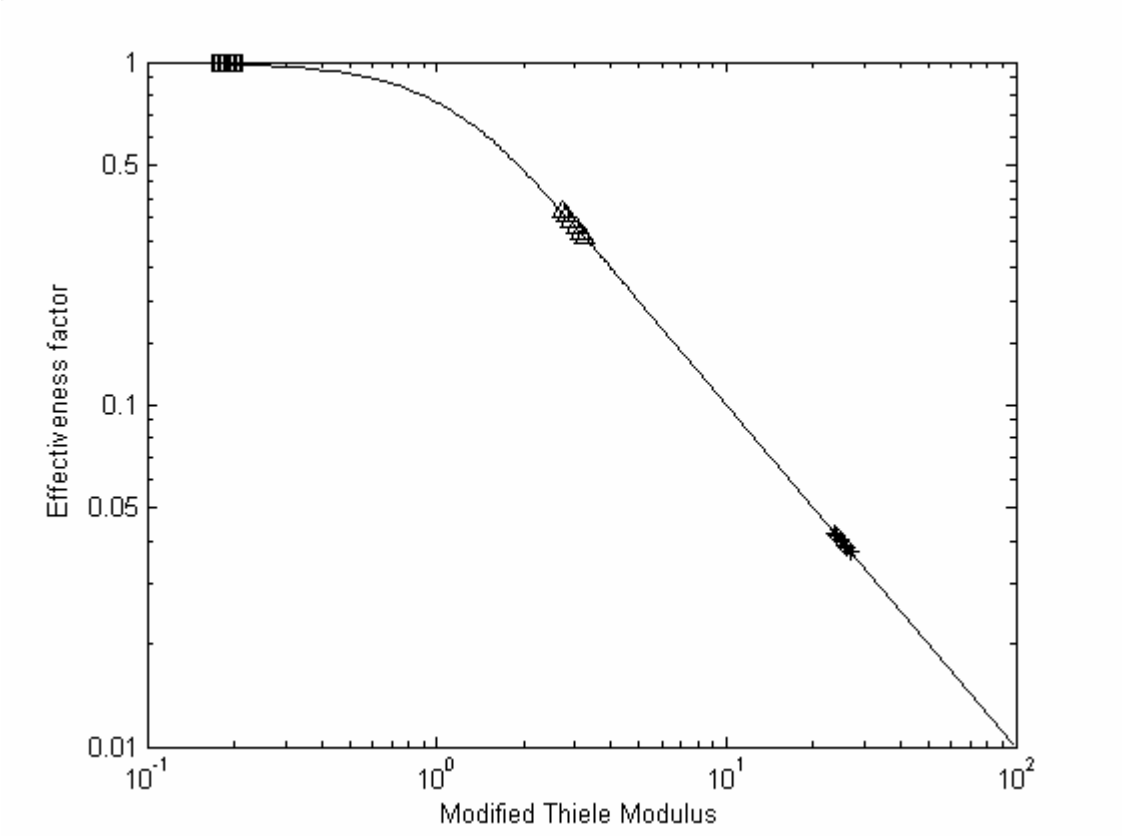

Figure 6b: Effectiveness factor versus modified Thiele Modulus. T = 500°C, (*) *m*-xylene, (Δ) *o*-xylene, and (□) *p*-xylene [Basis for Diffusion data - Hans et al.[33]].

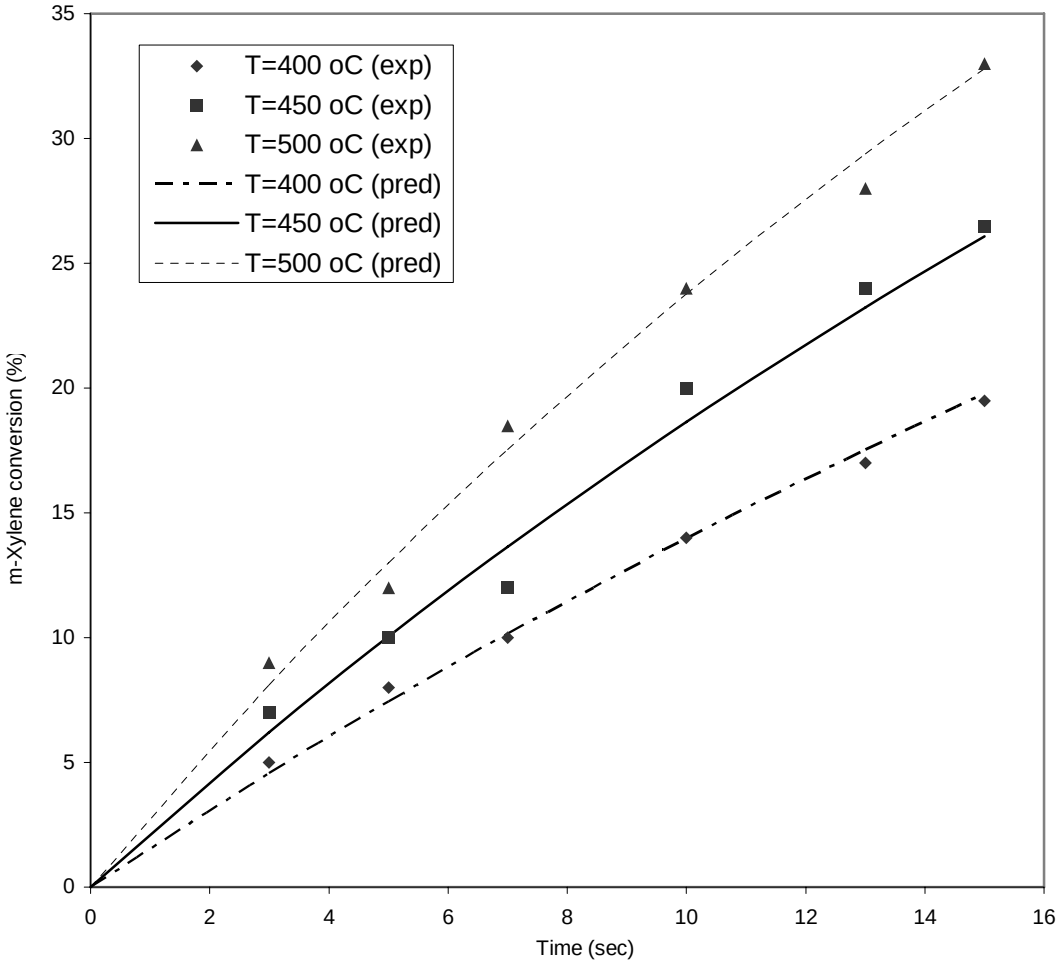

Figure 7a: Modeling *m*-Xylene conversion [Basis for Diffusion data - Hans et al.[33]]

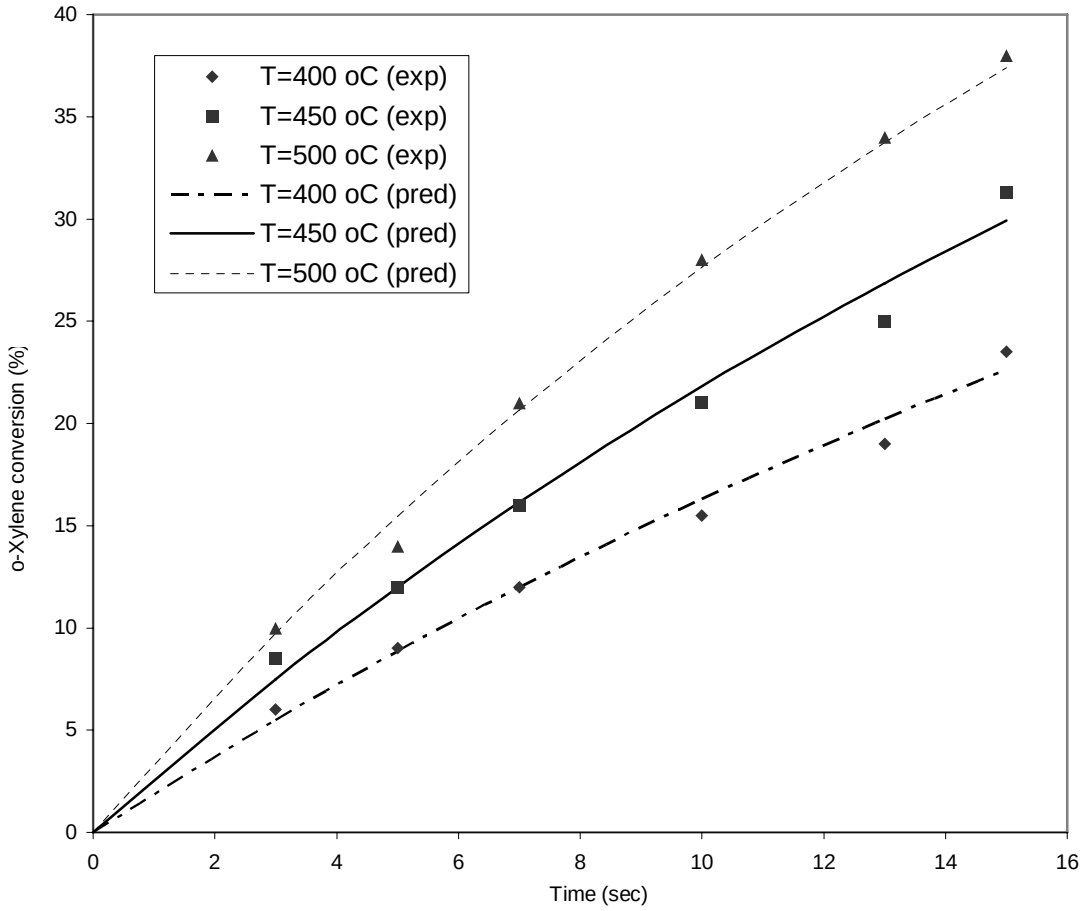

Figure 7b: Modeling *o*-Xylene conversion [Basis for Diffusion data - Hans et al.[33]]

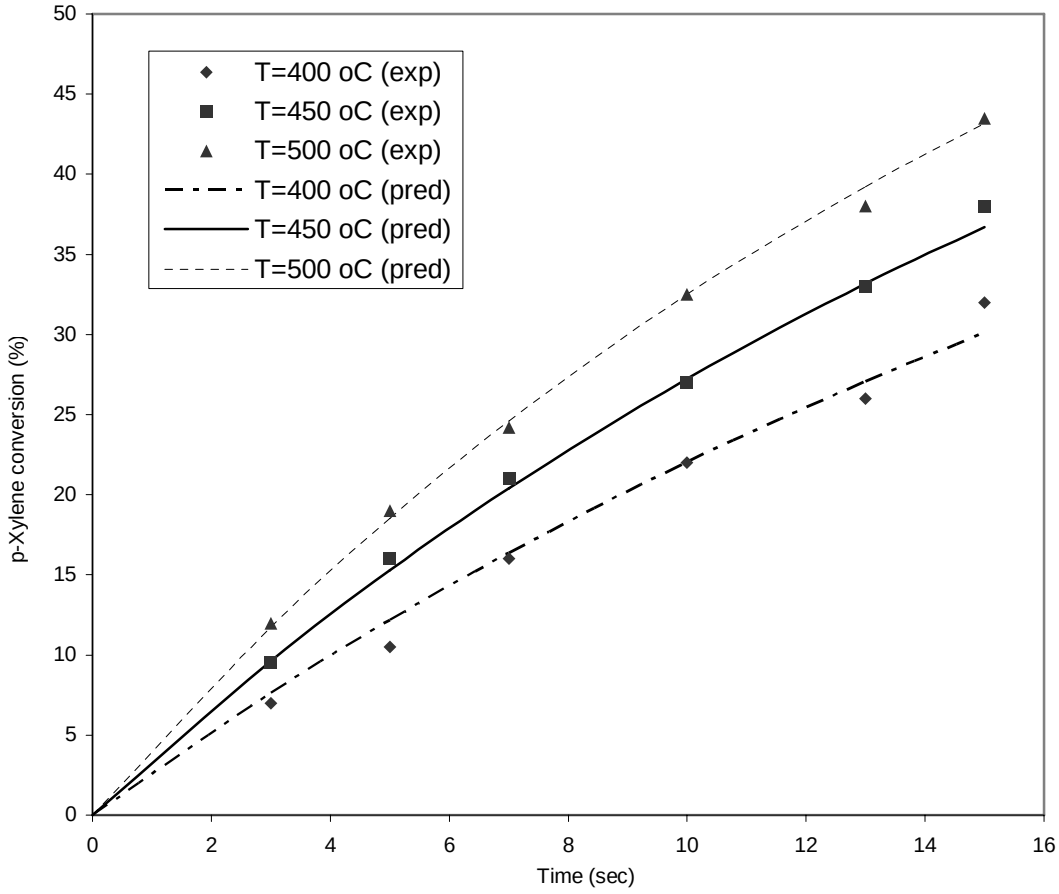

Figure 7c: Modeling *p*-Xylene conversion [Basis for Diffusion data - Hans et al.[33]]